microbial biotechnology

Open Access

Production of rebaudioside D from stevioside using a UGTSL2 Asn358Phe mutant in a multi-enzyme system

Liangliang Chen, Ruxin Cai, Jingyuan Weng, Yan Li* Honghua Jia, Kequan Chen, Ming Yan and Pingkai Ouyang

College of Biotechnology and Pharmaceutical Engineering, Nanjing Tech University, Nanjing 211800, China.

Summary

Rebaudioside D is a sweetener from *Stevia rebaudiana* with superior sweetness and organoleptic properties, but its production is limited by its minute abundance in *S. rebaudiana* leaves. In this study, we established a multi-enzyme reaction system with *S. rebaudiana* UDP-glycosyltransferases UGT76G1, *Solanum lycopersicum* UGTSL2 and *Solanum tuberosum* sucrose synthase StSUS1, achieving a two-step glycosylation of stevioside to produce rebaudioside D. However, an increase in the accumulation of rebaudioside D required the optimization of UGTSL2 catalytic activity towards glucosylation of rebaudioside A and reducing the formation of the side-product rebaudioside M2. On the basis of homology modelling and structural analysis, Asn358 in UGTSL2 was subjected to saturating mutagenesis, and the Asn358Phe mutant was used instead of wild-type UGTSL2 for bioconversion. The established multi-enzyme reaction system employing the Asn358Phe mutant produced 14.4 g l^{-1} (1.6 times of wild-type UGTSL2) rebaudioside D from 20 g l^{-1} stevioside after reaction for 24 h. This system is useful for large-scale rebaudioside D production and expands our understanding of the pathways involved in its synthesis.

Received 24 August, 2019; revised 17 December, 2019; accepted 13 January, 2020.
*For correspondence. E-mail: liyan@njtech.edu.cn; Tel. +86 25 58139919; Fax +86 25 58139905.
Microbial Biotechnology (2020) **13**(4), 974–983
doi:10.1111/1751-7915.13539
Funding Information
We greatly acknowledge the financial support from NSFC (21878155), PAPD, Qing Lan Project of Jiangsu Universities, the Six Talent Peaks Project in Jiangsu Province and the Jiangsu Synergetic Innovation Center for Advanced Bio-Manufacture.

Introduction

Rebaudioside D is a natural non-caloric sweetener with high sweetness (~350 times higher than sucrose) and a much less prolonged bitter taste than most other steviol glycosides (SGs) (Hellfritsch *et al*., 2012; Olsson *et al*., 2016). The United States Food and Drug Administration certified rebaudioside D as 'generally safe' in 2017 (FDA. GRN No. 715, Rebaudioside D.), allowing it to be used as a food additive in the food industry. To date, more than 35 different SGs have been isolated and analysed in terms of structure and characteristics (Wölwer-Rieck, 2012). Stevioside and rebaudioside A, both exist in the leaves of *Stevia rebaudiana*, are major ingredients of commercial *Stevia* sweeteners, and while the former is much cheaper due to its bitter aftertaste, the later has a more desirable taste and is consequently more expensive (Urban *et al*., 2015). Rebaudioside D performs even better than rebaudioside A and stevioside regarding perceived sweetness and taste intensity (Hellfritsch *et al*., 2012), and is considered a next-generation *Stevia* sweetener (Olsson *et al*., 2016). However, it is difficult to scale production by traditional extraction approaches due to its minute abundance in *Stevia* leaves (~0.4% w/w total dry weight; Jackson *et al*., 2009).

The biosynthetic pathways of SGs in *S. rebaudiana* have been clarified (Brandle and Telmer, 2007), and UDP-dependent glycosyltransferases (UGTs) play a key role (Mohamed *et al*., 2011). In addition to *S. rebaudiana*, UGTs with the catalytic capability for SG conversion have been identified in other species including *Solanum lycopersicum* (Prakash *et al*., 2014a, 2014b). UDP-glucose (UDPG), a relatively expensive sugar donor for UGTs, can be recycled by coupling with sucrose synthase, which provides a powerful approach for biocatalytic glycosylation process development (Schmölzer *et al*., 2016). Therefore, efficient enzymatic production of rebaudioside D by combining the activities of multiple UGTs is feasible.

Bioconversions of stevioside to rebaudioside A by UDP-glycosyltransferase UGT76G1 from *S. rebaudiana* (Wang *et al*., 2015) and rebaudioside A to rebaudioside D by UGTSL2 from *S. lycopersicum* (Chen *et al*., 2018) have been demonstrated in the presence of sucrose synthase from *Arabidopsis thaliana* or *Solanum tuberosum*. However, UGTSL2-mediated conversion of rebaudioside D to rebaudioside M2 (Prakash *et al*., 2014b;

Chen *et al*., 2018) can result in the formation of unwanted side-products such as rebaudioside M2, which decreases the accumulation of the rebaudioside D target compound. In the present study, on the basis of homology modelling and structural alignment, Asn358 close to the substrate-binding pocket of UGTSL2 was chosen for saturated mutagenesis to optimize the catalytic activity towards glycosylation of rebaudioside D, the substrate for generation of rebaudioside M2. The Asn358Phe mutant displayed improved activity for specific accumulation of the desired rebaudioside D, and a multi-enzyme system including Asn358Phe UGTSL2, UGT76G1 and StSUS1 was established and achieved enhanced production of rebaudioside D from stevioside.

Results and discussion

Synthesis of rebaudioside D from stevioside

In the present work, glucosyltransferase UGT76G1 from *S. rebaudiana*, UGTSL2 from *S. lycopersicum* and sucrose synthase StSUS1 from *S. tuberosum* were co-expressed in *E. coli* and used to catalyse the conversion of stevioside to rebaudioside D. In this reaction system, UGT76G1 and UGTSL2 are believed to be responsible for generating rebaudioside A from stevioside (Wang *et al*., 2015), and rebaudioside D from rebaudioside A (Chen *et al*., 2018) respectively (Fig. 1A). After 15 h of reaction, 20 g l^{-1} stevioside was almost exhausted, but rebaudioside A (11.9 g l^{-1}) was the main product, and the production of rebaudioside D (8.4 g l^{-1}) was poor (Fig. 1B). The main reason might be the low activity of UGTSL2 in the reaction. Accordingly, the site-saturated mutagenesis of UGTSL2 was carried out.

Target site identification in UGTSL2

In the glycosylation pathways of steviol in *S. rebaudiana*, UDP-glucosyltransferases act on different substrates, contributing to steviol glycoside diversity (Lim, 2005; Brandle and Telmer, 2007). Alignment of the amino acid sequences of *S. lycopersicum* derived glucosyltransferase UGTSL2 with another four *Stevia* glucosyltransferases, namely, UGT91D1, UGT74G1, UGT76G1 and UGT85C2, which could also catalyse the synthesis of SGs (Olsson *et al*., 2016), showed that the C-terminal domain is highly conserved, reflecting its major function as the UDPG binding domain (Fig. 2A), while the N-terminal domain responsible for binding steviol glycoside substrates is more variable. Phylogenetic analysis (Fig. S1) indicated that the sequence of UGTSL2 had closer homology with that of UGT91D1, though these five UGTs share relatively low sequence identity with each other (lower than 33%). From the UGTSL2 homology model with UDPG docked in the active site, 10 amino acid residues (His17, Thr138, 316Lys, Gln 320, His 335, Trp 338, Asn339, Ser340, Glu343 and Asp 359) were found to engage in hydrogen bonds with UDPG, indicating important functionalities (Fig. 2B). Among them, His17 appears to be the most important and conserved residue, which is positioned close to the hydroxyl groups of the acceptor and UDPG, similar to His22 in UGT71G1 (Shao *et al*., 2005) and His22 in UGT78G1 (Modolo *et al*., 2009). Another conserved residue, Asp359, is positioned close to His17 (6.0 Å) and forms two hydrogen bonds with UDPG. The site harbouring the most conserved residues was considered likely to have the greatest effect on the catalytic properties, especially enzyme activity and specificity. Therefore, Asn358, which is positioned very close to the substrate channel, was chosen as the target site for saturating mutagenesis.

Screening of UGTSL2 mutants

For preliminary screening, we compared the catalytic capacity of the UGTSL2 mutants for converting rebaudioside A to rebaudioside D using UDPG (Fig. S2). The results showed that three mutants (Asn358Ala, Asn358Leu and Asn358Met) exhibited higher activity than wild-type UGTSL2, while six mutants (Asn358Cys, Asn358Glu, Asn358Phe, Asn358Lys, Asn358Ile and Asn58Gly) displayed similar activity to UGTSL2, and the remaining mutants exhibited reduced activity compared with UGTSL2. Thus, these nine mutants were selected for further analysis.

Bioconversion of rebaudioside A to rebaudioside D was carried out using the nine UGTSL2 mutants and the wild-type enzyme by coupling to StSUS1. As indicated in Table 1, only the Asn358Phe mutant showed better catalytic activity towards rebaudioside A than wild-type UGTSL2 within 24 h. The order for rebaudioside A conversion was Asn358Phe>UGTSL2>Asn358Met>Asn358Cys>Asn358Leu>Asn358Ala>Asn358Lys>Asn358Gly>Asn358Glu>Asn358Ile. Among the mutants, Asn358Glu and Asn358Ile lost almost all enzyme activity.

Although the reaction rate of the Asn358Cys mutant was slow compared with wild-type UGTSL2, the conversion of rebaudioside A still reached 84.0% for 24 h, slightly lower than that of wild-type UGTSL2 (93.6%). However, the yield of rebaudioside D after 24 h using the Asn358Cys mutant (79.4%) was higher than that of the wild-type enzyme (64.7%) due to the generation of less rebaudioside M2, demonstrating the alteration in substrate selectivity for rebaudioside D. Interestingly, mutants Asn358Phe and Asn358Leu displayed opposite catalytic activities and substrate selectivities towards rebaudioside D. With mutant Asn358Phe, the yield of the main rebaudioside D product for 24 h (86.6%) was much

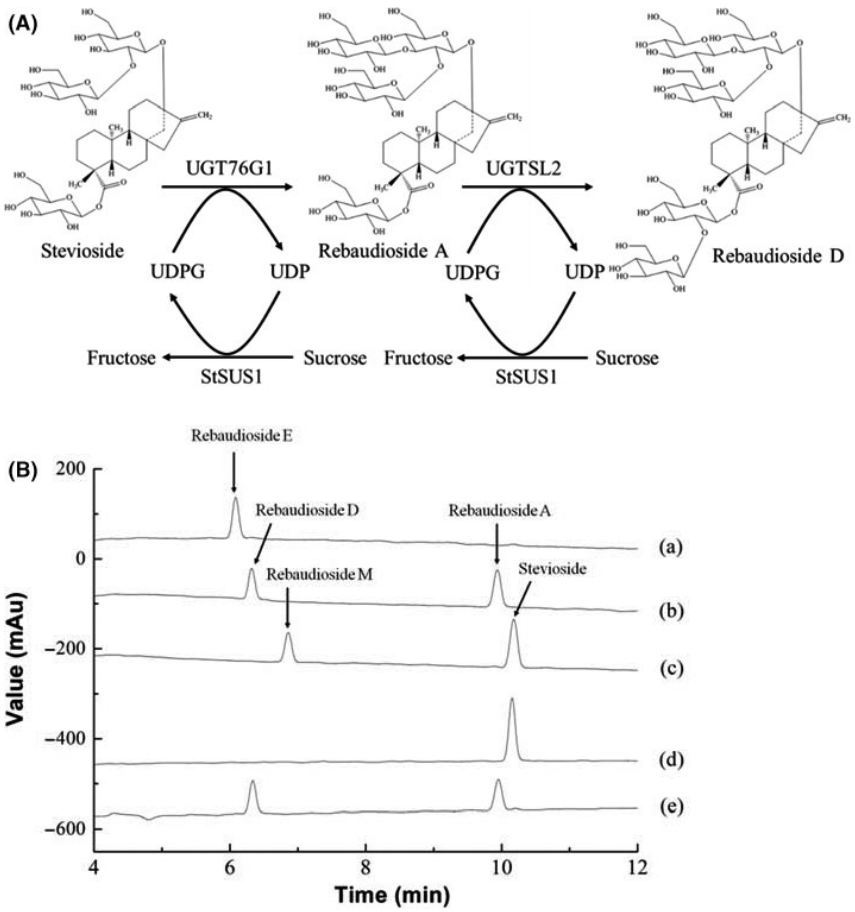

Fig. 1. A. Synthetic pathway of rebaudioside D from stevioside with UGT76G1, UGTSL2 and StSUS1.
B. Synthesis of rebaudioside D from stevioside with UGT76G1, UGTSL2 and StSUS1. Note: (a) 1.2 mM of rebaudioside E standard; (b) 1.2 mM of rebaudioside D and rebaudioside A standards; (c) 0.6 mM of rebaudioside M and 1.2 mM of stevioside standards; and (d,e) samples were taken after reaction of 0 h and 15 h respectively. A total of 161.4 mU ml^{-1} of UGT76G1, 33.0 mU ml^{-1} of UGTSL2 and 491.0 mU ml^{-1} of StSUS1 from the crude extract (6 mg ml^{-1} of total proteins) were incubated with 20 g l^{-1} of stevioside at 30°C and pH 7.2.

higher than that with native UGTSL2 (64.7%), and the formation of rebaudioside M2 side-product from rebaudioside D was strongly suppressed. Mutant Asn358Leu preferentially synthesized rebaudioside M2 over rebaudioside D, facilitating the conversion of rebaudioside D to rebaudioside M2 and resulting in less accumulation of rebaudioside D from rebaudioside A. Thus, mutant Asn358Phe was superior for the higher accumulation of rebaudioside D.

Differences in catalytic abilities between UGTSL2 and its mutant Asn358Phe, Asn358Cys and Asn358Leu were revealed by measuring their enzyme activities towards different substrates (Table 2). Mutant Asn358Phe had the highest specific activity towards rebaudioside A (9.4 ± 0.2 mU mg^{-1}) among the four enzymes, and lower activity towards rebaudioside D (2.4 ± 0.3 mU mg^{-1}) than those of wild-type UGTSL2 (12.1 ± 0.1 mU mg^{-1}) and mutant Asn358Leu (39.0 ± 0.3 mU mg^{-1}). Although the Asn358Cys mutant showed no activity towards rebaudioside D, its activity towards rebaudioside A was also low (5.4 ± 0.1 mU mg^{-1}).

Enhanced synthesis of rebaudioside D from stevioside

Multi-enzyme reactions for stevioside conversion were performed using wild-type and Asn358phe UGTSL2, UGT76G1 and StSUS1, prepared from *E. coli* BL21 (m358Phe-SUS1-C76G1) and *E. coli* BL21 (SL2-SUS1-C76G1) respectively. A significant increase in the specific activity of UGTSL2 was observed in the reaction mixtures including the Asn358Phe mutant (Table S1). In case of the modified enzyme activity pattern, the accumulation of rebaudioside D in the system containing the Asn358Phe mutant was enhanced to 12.9 g l^{-1} compared with wild-type UGTSL2 (7.4 g l^{-1}) after reaction for 16 h (Fig. 3). The molar yield of rebaudioside D was increased to

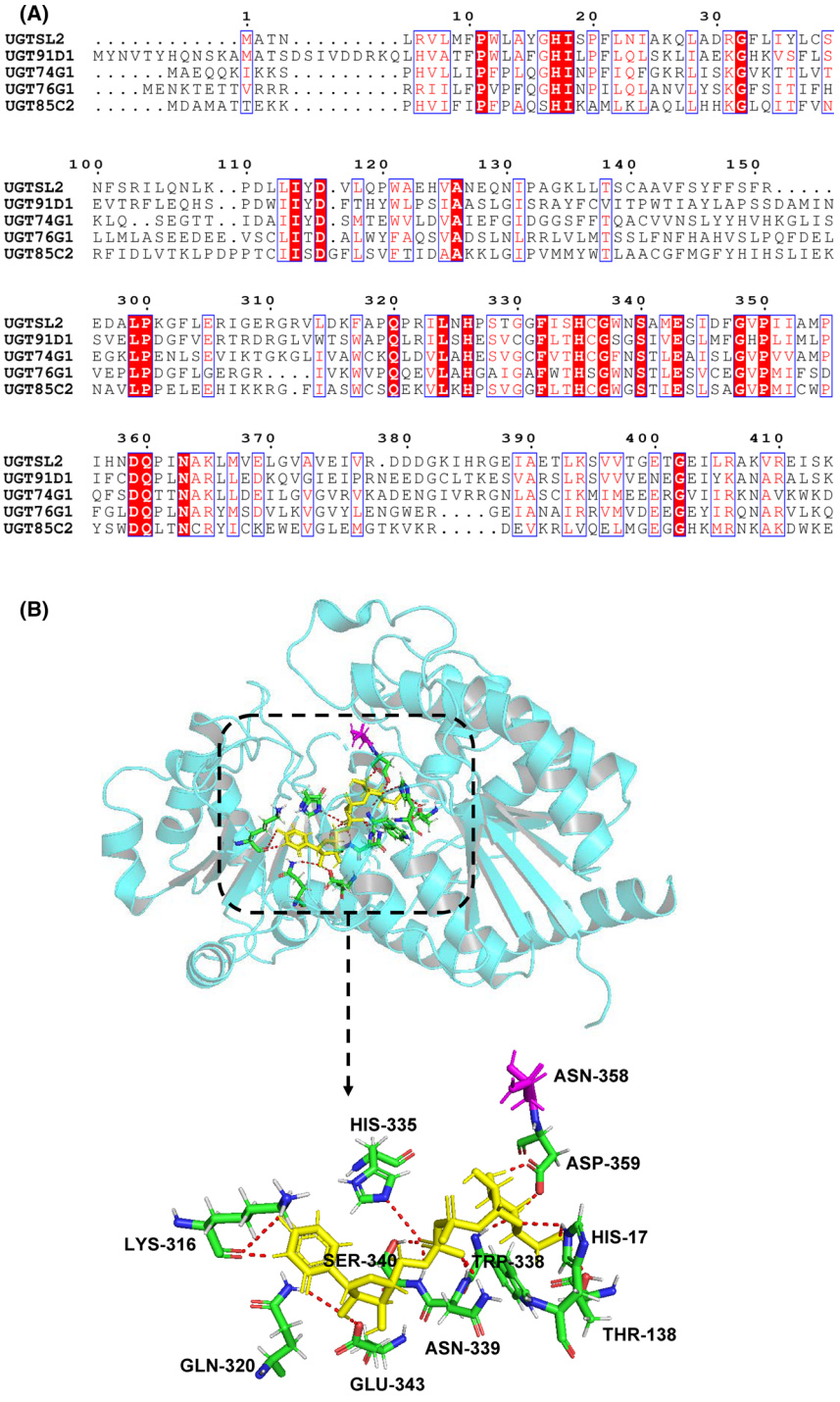

Fig. 2. A. Sequence alignment between UGTSL2 and other *Stevia* glucosyltransferases UGT91D1, UGT74G1, UGT76G1 and UGT85C2. B. UGTSL2 homology model with UDPG docked in the active sites. Note: The model shows the hydrogen bonds (red dashed line) between UDPG (yellow) and amino acid residues of UGTSL2. Asn358, purple.

51.3% (14.4 g l^{-1}) for the multi-enzyme system containing the Asn358Phe mutant, significantly higher than that with wild-type UGTSL2 (31.64%) when the reaction time was extended to 24 h. Under the above experiment conditions, no rebaudioside M2 was detected in ether mixture, probably because the concentrations of produced rebaudioside A were not as high as those (20 g l^{-1}) used in the rebaudioside A bioconversions (Table1).

Table 1. Bioconversion of rebaudioside A by wild-type UGTSL2 and its mutants

	RebA conversion (%)		RebD yield (%)		RebM2 yield (%)	
UGTSL2	12 h	24 h	12 h	24 h	12 h	24 h
Wild-type	90.8 ± 0.2	93.6 ± 0.3	84.4 ± 5.4	64.7 ± 0.7	3.7 ± 0.7	31.5 ± 1.2
Asn358Ala	16.5 ± 1.6	48.0 ± 2.6	18.7 ± 1.1	46.3 ± 1.4	N.D.	N.D.
Asn358Cys	52.6 ± 2.3	84.0 ± 1.1	51.0 ± 0.5	79.4 ± 1.4	0.4 ± 0.1	1.7 ± 0.3
Asn358Glu	1.0 ± 0.1	5.1 ± 1.3	0.9 ± 0.7	5.3 ± 1.8	N.D.	N.D.
Asn358Phe	94.3 ± 0.2	94.6 ± 0.5	92.5 ± 2.5	86.6 ± 3.4	0.4 ± 0.1	7.9 ± 1.2
Asn358Lys	25.1 ± 1.6	42.6 ± 2.7	22.5 ± 1.5	39.5 ± 2.4	0.4 ± 0.1	2.5 ± 0.5
Asn358Ile	0.4 ± 2.7	2.0 ± 1.1	0.1 ± 0.0	0.5 ± 0.3	N.D.	N.D.
Asn358Gly	14.5 ± 0.5	20.1 ± 1.1	12.2 ± 0.7	21.5 ± 0.9	N.D.	N.D.
Asn358Leu	32.1 ± 2.7	64.1 ± 2.9	24.2 ± 0.8	23.4 ± 0.4	7.8 ± 1.3	39.7 ± 0.5
Asn358Met	68.1 ± 3.0	88.6 ± 1.3	62.7 ± 2.2	80.1 ± 3.4	N.D.	6.3 ± 2.2

N.D., not detected; RebA, rebaudioside A; RebD, rebaudioside D; RebM2, rebaudioside M2. Results represent the means ± standard deviation of duplicates.

Table 2. The specific activities (mU mg^{-1}) of wild-type UGTSL2 and some mutants

	Specific activities (mU mg^{-1})	
Substrate	Rebsudioside A	Rebaudioside D
Wild-type UGTSL2	7.6 ± 0.4	12.1 ± 0.1
Asn358Phe	9.4 ± 0.2	2.4 ± 0.3
Asn358Cys	5.4 ± 0.1	0.0
Asn358Leu	5.1 ± 0.4	39.0 ± 0.3

Results represent the means ± standard deviation of duplicates.

K_m *values of wild-type UGTSL2 and mutant Asn358Phe*

The K_m values of mutant Asn358Phe for rebaudioside A (0.44 ± 0.01 mM) and rebaudioside D (0.07 ± 0.01 mM) were much lower than those of wild-type UGTSL2 (0.87 ± 0.07 mM, 0.31 ± 0.01 mM), which indicated increased affinity for the two tested SGs compared with wild-type UGTSL2 (Table 3). Notably, the K_m value of mutant Asn358Phe for rebaudioside D was less than that of native UGTSL2, but its enzymatic activity towards rebaudioside D was relatively low.

Channels of UDPG in wild-type UGTSL2 and Asn358Phe mutant

On the basis of the homology model of UGTSL2 and UDPG, a small difference was evident around the mutated site, with the conserved Ser258 forming a new hydrogen bond with UDPG, which may strengthen enzyme-substrate interactions. The molecular channel for substrate entry was detected using CAVER with a minimal probe radius of 0.7 and the channel spans between the glycosyl donor UDPG. On the basis of the Avg_throughput parameter, we analysed the main channels in wild-type and Asn358Phe mutant UGTSL2 enzymes (Fig. 4). The channel was altered dramatically

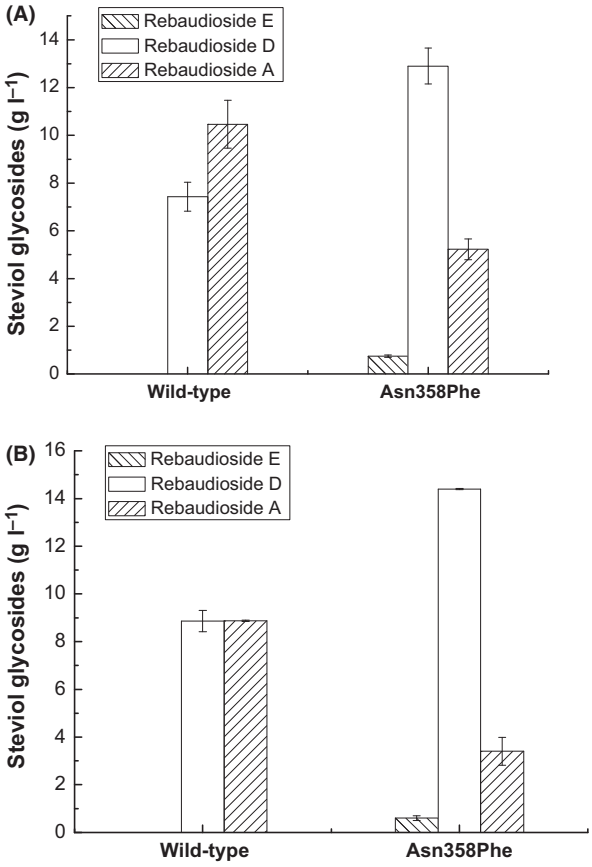

Fig. 3. Synthesis of rebaudioside D from stevioside with UGT76G1, StSUS1 and wild-type UGTSL2 or the mutant Asn358Phe. Note: Samples were taken after reaction of 16 h (A) and 24 h (B) from the mixtures in which 20 g l^{-1} of stevioside and the crude extracts were incubated at 30°C and pH 7.2, with 134.5 mU ml^{-1} of UGT76G1, 27.5 mU ml^{-1} of UGTSL2 and 409.0 mU ml^{-1} of StSUS1, or 65.0 mU ml^{-1} of UGT76G1, 60.5 mU ml^{-1} of Asn358Phe and 347.0 mU ml^{-1} of StSUS1 respectively. Results are means of duplicate experiments, and error bars represent ± standard deviation.

Table 3. K_m (mM) values of the purified wild-type UGTSL2 and Asn358Phe mutant

	K_m (mM)	
Substrate	Rebsudioside A	Rebaudioside D
Wild-type UGTSL2	0.87 ± 0.07	0.31 ± 0.01
Asn358Phe	0.44 ± 0.01	0.07 ± 0.01

Results represent the means ± standard deviation of triplicates.

in the mutant, in terms of its direction, length and diameter. After mutation, the number of amino acid residues forming the channel increased from 10 (Glu259, Ser258, Glu45, Ile47, Lys316, Gly257, His335, Tyr260, Glu292 and Gly291) to 15 (Glu259, Ser258, Ala14, Tyr15, Gly257, Phe358, His335, Gly16, Tyr260, His17, Asn87, Trp12, Leu118, Ser340 and Gly337), the length of the channel increased from 15 Å to 19.3 Å, and the diameter of the channel also decreased slightly (Fig. S3). Phe358 is present in the channel of the Asn358Phe mutant and brings greater hydrophobicity, possibly improving local structural stability (Fig. S4).

The Asn358Phe mutation would be one of the mutants that fine-tuned the channel and the cavity for substrate binding. The catalytic ability of the mutant was improved for accumulation of rebaudioside D from stevioside in the multi-enzyme reaction involving glucosyltransferases UGT76G1 and UGTSL2, and sucrose synthase StSUS1. This work addresses some of the issues associated with the multi-step glycosylation of SGs and demonstrates a changed substrate specificity and the enhanced target production on the basis of the site saturation mutagenesis.

Experimental procedures

Plasmids and strains

The optimized genes encoding a fusion protein of 3′-phosphoadenosine-5′-phosphatase (NCBI Reference Sequence: 948728) and UGT76G1 (NCBI Reference Sequence: LC037193) in pET-C76G1 (Chen *et al*., 2017) and StSUS1 (NCBI Reference Sequence: LC430937) in pRSF-SL2-SUS1 (Chen *et al*., 2018) were subcloned into the NdeI/XhoI and NcoI/EcoRI sites of pCDFDuet-1 (Novagen, Madison, WI, USA), respectively, resulting the plasmid pCDF-C76G1-SUS1. Plasmid pRSF-SL2-SUS1 (Chen *et al*., 2018) served as a template for site-directed mutagenesis of UGTSL2 (NCBI Reference Sequence: XP_004250485.1) to mutate Asn358 to other 19 amino acid residues. The resulting plasmids carrying wild-type or mutant UGTSL2 were transformed into the *Escherichia coli* BL21 (DE3) strain (TransGen Biotech, Beijing, China), with or without pCDF-C76G1-SUS1. All plasmids and strains used in this study are listed in Table S2.

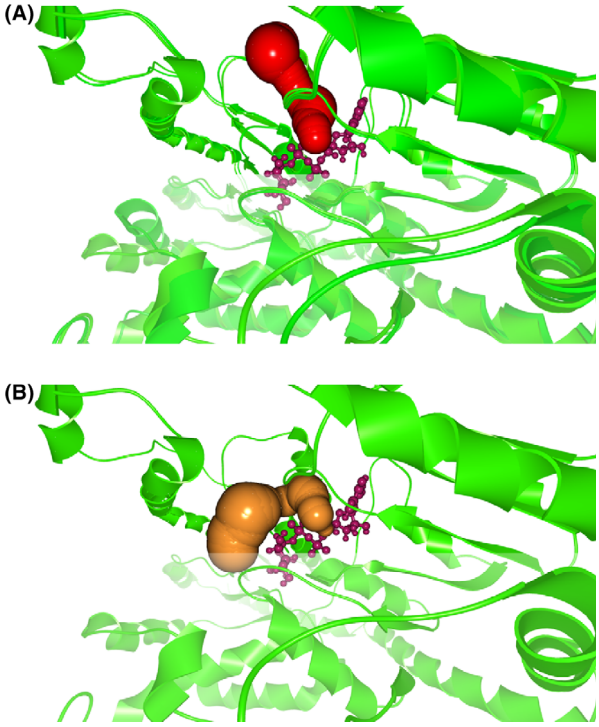

Fig. 4. Channel analysis of wild-type UGTSL2 (A) and the mutant Asn358Phe (B). Note: purple stick model was UDPG.

Protein sequence and structure analysis

The amino acid sequence of glucosyltransferase UGTSL2 from *S. lycopersicum*, used for enzymatic conversion of rebaudioside A to rebaudioside D (Chen *et al*., 2018), was aligned with four glucosyltransferases from *S. rebaudiana* (UGT91D1, UGT74G1, UGT76G1 and UGT85C2) using Clustal X (Table S3; Heringa, 1999). A phylogenetic tree was constructed with MEGA 7.0 (Kumar *et al*., 2016) by using the neighbour-joining algorithm (Saitou and Nei, 1987). A three-dimensional structural model of UGTSL2 was obtained from the Robetta server (http://robetta.bakerlab.org/) and evaluated by PROCHECK (http://servicesn.mbi.ucla.edu/PROCHECK/; Laskowski *et al*., 1993). Model refinement and docking of ligands to UGTSL2 were performed using YASARA (Krieger and Vriend, 2014). Calculation, analysis and visualization of access tunnels in the protein structure were carried out by CAVER (Chovancova *et al*., 2012; Kozlikova *et al*., 2014; Jurcik *et al*., 2018).

Site-directed mutagenesis

Using pRSF-SL2-SUS1 as a template, mutation was carried out using a Mut ExpressR II Fast Mutagenesis Kit V2 (Vazyme Biotech Co., Ltd, Nanjing China). Reactions (50 μl) contained ≤ 1 ng template plasmid in 1× Max buffer, 0.2 mM dNTP Mix, 0.4 μM primers and 1 U

Phanta Max Super-Fidelity DNA Polymerase. After predenaturation at 95°C for 30 s, thermal cycling was performed at 95°C for 15 s, 70°C for 15 s and 72°C for 3 min (30 cycles), followed by a final extension at 72°C for 5 min. DpnI (10 U) was then added and incubated at 37°C for 1 or 2 h for template digestion, and Exnase II was added and incubated at 37°C for 30 min for cyclization of linearized plasmids (PCR products), which were subsequently transformed into competent *E. coli* BL21 (DE3) cells. After culturing, plasmids were isolated and sequenced by GenScript (Nanjing, China) to confirm introduction of the desired mutations. Primers used to generate individual mutants are listed in Table S4.

Enzyme expression in E. coli

To express glycosyltransferase and sucrose synthase, recombinant *E. coli* BL21 (DE3) cells were incubated in 100 ml of fresh auto-induction medium (15 g l^{-1} of tryptone, 25 g l^{-1} of yeast extract, 10 g l^{-1} of NaCl, 2 g l^{-1} of glucose and 0.5 g l^{-1} of lactose) supplemented with antibiotics (50 mg l^{-1} kanamycin, and 40 mg l^{-1} streptomycin if needed) at 30°C and 200 rpm until OD_{600} reached approximately 0.2. Afterwards, cultures were kept at 25°C for a further 22 h with shaking at 200 rpm. The cells were harvested by centrifugation at 5289 × *g*, 4°C for 5 min, and washed twice and resuspended with 50 mM potassium phosphate buffer (pH 7.2). The cell suspension was disrupted for 10 min by an Ultrasonic Cell Disruptor JY92-IIN (SCIENTZ, Ningbo, China). The lysate was centrifuged at 6010 × *g*, 4°C for 20 min to obtain the supernatant as the crude extract. Total protein concentrations were measured by the Bradford assay, using bovine serum albumin (BSA) as a standard (Bradford, 1976).

Enzyme activity assay

The glucosyltransferase activity was measured in a total volume of 3 ml containing following components: 1 mg of total protein from the crude extract, 1.2 mM stevioside (or rebaudioside A or rebaudioside D), 2 mM UDP-glucose, 3 mM $MgCl_2$ and 50 mM potassium phosphate buffer (pH 7.2). After 30 min of incubation at 30°C, samples (500 μl) were removed, heated at 95°C for 10 min to quench the reaction and centrifuged at 13 523 × *g* for 1 min. The concentrations of SGs in supernatants were determined by high-performance liquid chromatography (HPLC; described below). One unit (U) of glycosyltransferase activity was defined as the amount of enzyme that produced 1 μmol of product (rebaudioside A or rebaudioside D or rebaudioside M2) from the corresponding substrate (stevioside or rebaudioside A or rebaudioside D) per min under the given assay conditions (Chen *et al.*, 2018).

The sucrose synthase activity was measured in the cleavage direction. The reaction mixture contained 6 mg of total protein from the crude extract, 500 mM sucrose, 10 mM UDP and 50 mM potassium phosphate buffer (pH 7.2) in a final volume of 3 ml. The mixture was incubated at 30°C, and samples (500 μl) were taken periodically. The samples were heated at 95°C for 10 min to quench the reaction and centrifuged at 13 523 × *g* for 1 min. Supernatants were analysed using the 3,5-dinitrosalicylic acid (DNS) method (Miller, 1959). One unit (U) of sucrose synthase activity was defined as the amount of enzyme that produced 1 μmol of fructose from sucrose per min under the given assay conditions.

Purification of glucosyltransferase UGTSL2

Purification of the recombinant glucosyltransferase UGTSL2 was performed with the AKTA Primer Plus (GE Healthcare Bio-science, Uppsala, Sweden) using a high affinity Ni-charged resin FF prepacked column (GenScript, Nanjing, China). The mobile phase A was 500 mM NaCl and 10% glycerine (v/v) in 20 mM sodium phosphate buffer (pH 7.2), and the mobile phase B was the mobile phase A modified with 250 mM imidazole. The resin column was loaded with the crude extract (20 ml) after the column was balanced with mobile phase A, and then, it was washed by mobile phase A again until no proteins dropped. Subsequently, gradient elution with the increase of the concentration of imidazole for washing the target protein was as follows: 0–30 min, from (0% B) to (20% B); 30–40 min, keeping (20% B); 40–70 min, from (20% B) to (100% B); and 70–90 min, keeping (100% B). The flow rate was 1 ml min^{-1}. The target protein UGTSL2 was eluted down under 150 mM imidazole and then analysed using sodium dodecyl sulfate-polyacrylamide gel electrophoresis (SDS-PAGE; Schägger and Jagow, 1987).

Enzyme kinetic evaluation

Glycosylation reactions were carried out at 30°C in a total volume of 500 μl, containing 50 μg of the purified wild-type UGTSL2 or Asn358Phe mutant from the crude extract, different concentrations of rebaudioside A or rebaudioside D (0.1–1.0 mM), 2 mM UDP-glucose, 3 mM $MgCl_2$ and 50 mM potassium phosphate buffer (pH 7.2). After incubation for every hour, samples were removed, heated at 95°C for 10 min to quench the reaction and centrifuged at 13 523 × *g* for 1 min. The concentrations of SGs in supernatants were determined by HPLC (described below). Glycosylation rates were calculated as μmol of glucosides formed per reaction time per amount of protein

(μmol min^{-1} mg^{-1}). The Michaelis–Menten kinetic model was fitted to glycosylation rates versus substrate concentrations, and the K_m of UGTSL2 for rebaudioside A or rebaudioside D was calculated according to the Lineweaver–Burk plot (Lineweaver and Burk, 1934).

Mutant screening

In the preliminary screening of UGTSL2 mutants with improved activity for production of rebaudioside D, recombinant *E. coli* colonies carrying the plasmid harbouring genes encoding wild-type or mutant UGTSL2, and StSUS1 were picked and placed in a 96-deepwell plate (The volume is 1.2 ml for each well) containing 300 μl of Luria–Bertani (LB) media (10 g l^{-1} tryptone, 5 g l^{-1} yeast extract, 10 g l^{-1} NaCl) with kanamycin (50 mg l^{-1}). Cells were grown overnight at 37°C with shaking at 200 rpm, and a 50 μl aliquot was used to inoculate 400 μl of fresh LB media with kanamycin in another 96-deepwell plate. After incubation at 37°C with shaking at 200 rpm for 2 h, 450 μl of LB media with kanamycin and Isopropyl β-D-Thiogalactoside (IPTG, 0.2 mM final concentration) were added to the above cultures, which were then transferred to 30°C and incubated with shaking at 200 rpm for 24 h for recombinant gene expression. Cells were pelleted by centrifugation (766 × *g*, 4°C, 10 min) and resuspended in two volumes of TRIS-HCl buffer (20 mM, pH 7.2). An appropriate amount of lysozyme was added, and samples were incubated at room temperature for 2 h. Following centrifugation at 766 × g, 4°C for 10 min, clear supernatants were transferred to a 96-deepwell plate and the enzyme activities of mutants were assessed in assays containing 75 μg of total protein from the crude extract, 1.2 mM rebaudioside A, 2 mM UDPG and 3 mM $MgCl_2$ in TRIS-HCl buffer (20 mM, pH 7.2) in a total volume of 500 μl. Reactions were performed at 30°C for 1 h.

In the second screening of UGTSL2 mutants, the abilities of enzymatic synthesis of rebaudioside D from rebaudioside A of UGTSL2 or mutants were measured coupling StSUS1. The reaction system was as below.

Biosynthesis of rebaudioside D

For biosynthesis of rebaudioside D by glucosyltransferases coupled to sucrose synthase, reaction mixtures (20 ml) contained 20 g l^{-1} of stevioside or rebaudioside A, 60 g l^{-1} of sucrose, 120 mg of total protein from the crude extract, 3 mM $MgCl_2$ and potassium phosphate buffer (50 mM, pH 7.2). Reactions were incubated at 30°C for 24 h with shaking at 200 rpm. A control experiment was performed under the same conditions using the crude extract prepared from *E. coli* transformants containing empty plasmid pRSFDuet-1.

HPLC analysis

Samples from the above reactions were taken and heated at 95°C for 10 min for determination by HPLC using an UltiMate 3000 HPLC system (Dionex China Limited, Beijing, China) as descripted previously (Chen *et al*., 2018). Rebaudioside D (97.6%) and rebaudioside E (91.0%) standards for HPLC were purchased from Yuanye Bio-Technology (Shanghai, China) and ChromaDex Inc. (USA) respectively. Stevioside (95.0%), rebaudioside A (98.0%), rebaudioside M (95.0%) and rebaudioside M2 (95.0%) standards for HPLC were kindly provided by Xinghua GL Stevia Co., Ltd (China). The yields and conversions were calculated as follows.

When rebaudioside A was used as the substrate in the reactions:

$$\text{Rebaudioside D yield}\,(\%) = C(\text{RD})/C(\text{RA\_ini})$$

$$\text{Rebaudioside M2 yield}\,(\%) = C(\text{RM2})/C(\text{RA\_ini})$$

$$\text{Rebaudioside A conversion}\,(\%) = C(\text{RA})/C(\text{RA\_ini})$$

When stevioside was used as the substrate in the reactions:

$$\text{Rebaudioside D yield}\,(\%) = C(\text{RD})/C(\text{St\_ini})$$

$$\text{Rebaudioside A yield}\,(\%) = C(\text{RA})/C(\text{St\_ini})$$

$$\text{Stevioside conversion}\,(\%) = C(\text{St})/C(\text{St\_ini})$$

where *C*(RA_ini) and *C*(St_ini) represent the initial molar concentrations of rebaudioside A and stevioside, respectively, and *C*(RD), *C*(RM2) and *C*(RA) represent the increased molar concentrations of rebaudioside D, rebaudioside M2 and rebaudioside A, respectively, after reaction.

Acknowledgements

We greatly acknowledge the financial support from NSFC (21878155), PAPD, Qing Lan Project of Jiangsu Universities, the Six Talent Peaks Project in Jiangsu Province and the Jiangsu Synergetic Innovation Center for Advanced Bio-Manufacture.

Conflict of interests

The authors declare that they have no competing interests.

Author contributions

LC and YL conceived and designed the study. LC, RC and JW performed the experiments and analysed the data. LC wrote the manuscript. HJ, KC, MY and PO reviewed and edited the manuscript. All authors read and approved the manuscript.

References

Bradford, M.M. (1976) A rapid and sensitive method for the quantitation of microgram quantities of protein utilizing the principle of protein-dye binding. *Anal Biochem* **72:** 248–254.

Brandle, J.E., and Telmer, P.G. (2007) Steviol glycosides biosynthesis. *Phytochemistry* **68:** 1855–1863.

Chen, L., Sun, P., Li, Y., Yan, M., Xu, L., Chen, K., and Ouyang, P. (2017) A fusion protein strategy for soluble expression of *Stevia* glycosyltransferase UGT76G1 in *Escherichia coli*. *3*. *Biotech* **7:** 356–363.

Chen, L., Sun, P., Zhou, F., Li, Y., Chen, K., Jia, H., *et al*. (2018) Synthesis of rebaudioside D, using glycosyltransferase UGTSL2 and *in situ* UDP-glucose regeneration. *Food Chem* **259:** 286–291.

Chovancova, E., Pavelka, A., Benes, P., Strnad, O., Brezovsky, J., Kozlikova, B., *et al*. (2012) CAVER 3.0: A tool for the analysis of transport pathways in dynamic protein structures. *PLoS Comput Biol* **8:** e1002708–e1002719.

FDA. GRN No. 715, Rebaudioside D. URL https://www.accessdata.fda.gov/scripts/fdcc/index.cfm?set=GRASNotices&xml:id=715.

Hellfritsch, C., Brockhoff, A., Stähler, F., Meyerhof, W., and Hofmann, T. (2012) Human psychometric and taste receptor responses to steviol glycosides. *J Agric Food Chem* **60:** 6782–6793.

Heringa, J. (1999) Two strategies for sequence comparison: profile-preprocessed and secondary structure-induced multiple alignment. *Comput Chem* **23:** 341–364.

Jackson, A.U., Tata, A., Wu, C., Perry, R.H., Haas, G., West, L., and Cooks, R.G. (2009) Direct analysis of *Stevia* leaves for diterpene glycosides by desorption electrospray ionization mass spectrometry. *Analyst* **134:** 867–874.

Jurcik, A., Bednar, D., Byska, J., Marques, S.M., Furmanova, K., Daniel, L., *et al*. (2018) CAVER Analyst 2.0: analysis and visualization of channels and tunnels in protein structures and molecular dynamics trajectories. *Bioinformatics* **34:** 3586–3588.

Kozlikova, B., Sebestova, E., Sustr, V., Brezovsky, J., Strnad, O., Daniel, L., *et al*. (2014) CAVER Analyst 1.0: graphic tool for interactive visualization and analysis of tunnels and channels in protein structures. *Bioinformatics* **30:** 2684–2686.

Krieger, E., and Vriend, G. (2014) YASARA View—molecular graphics for all devices—from smartphones to workstations. *Bioinformatics* **30:** 2981–2982.

Kumar, S., Stecher, G., and Tamura, K. (2016) MEGA7: molecular evolutionary genetics analysis version 7.0 for bigger datasets brief communication. *Mol Biol Evol* **33:** 1870–1874.

Laskowski, R.A., Macarthur, M.W., Moss, D.S., and Thornton, J.M. (1993) PROCHECK: a program to check the stereochemical quality of protein structures. *J Appl Crystallogr* **26:** 283–291.

Lim, E.K. (2005) Plant glycosyltransferases: their potential as novel biocatalysts. *Chem Eur* **11:** 5486–5494.

Lineweaver, H., and Burk, D. (1934) The determination of enzyme dissociation constants. *J Am Chem Soc* **56:** 658–666.

Miller, G.L. (1959) Use of dinitrosalicylic acid reagent for determination of reducing sugar. *Anal Chem* **31:** 426–428.

Modolo, L.V., Li, L.N., Pan, H.Y., Blount, J.W., Dixon, R.A., and Wang, X.Q. (2009) Crystal structures of glycosyltransferase UGT78G1 reveal the molecular basis for glycosylation and deglycosylation of (iso)flavonoids. *J Mol Biol* **392:** 1292–1302.

Mohamed, A.A.A., Ceunen, S., Geuns, J.M.C., Ende, W.V., and Ley, M.D. (2011) UDP-dependent glycosyltransferases involved in the biosynthesis of steviol glycosides. *J Plant Physiol* **168:** 1136–1141.

Olsson, K., Carlsen, S., Semmler, A., Simón, E., Mikkelsen, M. D., and Møller, B. L. (2016) Microbial production of next-generation stevia sweeteners. *Microb Cell Fact* **15:** 207–222.

Prakash, I., Bunders, C., Devkota, K.P., Charan, R.D., Ramirez, C., Parikh, M., and Markosyan, A. (2014a) Isolation and structure elucidation of rebaudioside D2 from bioconversion reaction of rebaudioside A to rebaudioside D. *Nat Prod Commun* **9:** 1135–1138.

Prakash, I., Bunders, C., Devkota, K.P., Charan, R.D., Ramirez, C., Priedemann, C., and Markosyan, A. (2014b) Isolation and characterization of a novel rebaudioside M isomer from a bioconversion reaction of rebaudioside A and NMR comparison studies of rebaudioside M isolated from *Stevia rebaudiana* Bertoni and *Stevia rebaudiana Morita*. *Biomolecules* **4:** 374–389.

Saitou, N., and Nei, M. (1987) The neighbor-joining method: a new method for reconstructing phylogenetic trees. *Mol Biol Evol* **4:** 406–425.

Schägger, H., and Jagow, G.V. (1987) Tricine-sodium dodecyl sulfate-polyacrylamide gel electrophoresis for the separation of proteins in the range from 1 to 100 kDa. *Anal Biochem* **166:** 368–379.

Schmölzer, K., Gutmann, A., Diricks, M., Desmet, T., and Nidetzky, B. (2016) Sucrose synthase: A unique glycosyltransferase for biocatalytic glycosylation process development. *Biotechnol Adv* **34:** 88–111.

Shao, H., He, X.Z., Achnine, L., Blount, J.W., Dixon, R.A., and Wang, X.Q. (2005) Crystal structures of a multifunctional triterpene/flavonoid glycosyltransferase from *Medicago truncatula*. *Plant Cell* **17:** 3141–3154.

Urban, J.D., Carakostas, M.C., and Taylor, S.L. (2015) Steviol glycoside safety: are highly purified steviol glycoside sweeteners food allergens? *Food Chem Toxicol* **75:** 71–78.

Wang, Y., Chen, L., Li, Y., Li, Y., Yan, M., Chen, K., *et al*. (2015) Efficient enzymatic production of rebaudioside A from stevioside. *Biosci Biotechnol Biochem* **80:** 1–7.

Wölwer-Rieck, U. (2012) The leaves of *Stevia rebaudiana* (Bertoni), their constituents and the analyses thereof: a review. *J Agric Food Chem* **60:** 886–895.

Supporting information

Additional supporting information may be found online in the Supporting Information section at the end of the article.

Fig. S1. Phylogenetic tree constructed using the amino acid sequences of UGTSL2 and other four Stevia glucosyltransferases.

Fig. S2. Comparison of the catalytic capabilities of the Asn358 mutants of UGTSL2.

Fig. S3. Analysis of the channel diameter and length of UGTSL2 before (red) and after (yellow) mutation.

Fig. S4. Analysis of the hydrophobicity of amino acid residues in channels of UGTSL2 before (A) and after (B) mutation.

Table S1. The specific activities of each enzyme that was used in the multi-enzyme system.

Table S2. Plasmids and strains used in this study.

Table S3. UniprotKB accession number of the protein sequences used in the multiple alignment.

Table S4. Primers used for site-directed mutagenesis.

